TR/71 APRIL 1977

THE BERGMAN KERNEL METHOD FOR THE NUMERICAL CONFORMAL MAPPING OF SIMPLY CONNECTED DOMAINS

by

D. LEVIN, N. PAPAMICHAEL and A. SIDERIDIS.

ABSTRACT

A numerical method for the conformal mapping of simply-connected domains onto the unit disc is considered. The method is based on the use of the Bergman kernel function of the domain. It is shown that, for a successful application, the basis of the series representation of the kernel must include terms that reflect the main singular behaviour of the kernel in the complement of the domain.

1. Introduction

Let Ω be a bounded simply-connected domain with boundary $\partial\Omega$ in the complex z-plane (z=x+iy) and let t be a fixed point in Ω. Consider the Bergman kernel function K(z;t) of Ω. This function is completely characterized by its reproducing property

$$g(t) = \iint_{\Omega} \overline{K(z;t)} g(z) dxdy = (g(z), K(z;t)), g(z) \in L^2(\Omega), \tag{1.1}$$

where $L^2(\Omega)$ is the Hilbert space of all square integrable analytic functions in Ω and $(g_1(z), g_2(z))$ denotes the inner product

$$(g_1(z), g_2(z)) = \iint_{\Omega} g_1(z) \overline{g_2(z)} dxdy, \tag{1.2}$$

of $L^2(\Omega)$.

It is well-known that:

(i) If $\{\phi_j(z)\}_{j=1}^{\infty}$ is any orthonormal basis of $L^2(\Omega)$ then K(z;t) has the infinite series expansion

$$K(z;t) = \sum_{j=1}^{\infty} \phi_j(z) \overline{\phi_j(t)}, \tag{1.3}$$

which, for fixed t, converges uniformly and absolutely in any closed domain which is entirely within Ω; Nehari (1952;p.250).

(ii) If

$$w = f(z), \tag{1.4}$$

is the mapping function which maps Ω conformally onto the unit disc $|w| < 1$, in such a way that

$$f(t) = 0 \text{ and } f'(t) > 0, \qquad t \in \Omega, \tag{1.5}$$

then

$$f(z) = \left\{ \frac{\pi}{K(t,t)} \right\}^{\frac{1}{2}} \int_t^z K(\zeta;t) d\zeta ; \tag{1.6}$$

Nehari (1952;p.252)

Given a complete set of functions $\{v_j(z)\}_{j=1}^{\infty}$ of $L^2(\Omega)$, the results (i) and (ii) suggest the following procedure for obtaining a numerical approximation to the mapping function f(z). The set $\{v_j(z)\}_{j=1}^{N}$ is orthonormalized by means of the Gram-Schmidt process, to give the set of orthonormal functions $\{\phi_j(z)\}_{j=1}^{N}$. The series (1.3) is then truncated after N terms to give the approximation

$$K_N(z;t) = \sum_{j=1}^{N} \phi_j(z)\overline{\phi_j(t)}, \tag{1.7}$$

to K(z;t) and finally equation (1.6) is used to give the approximation

$$f_N(z) = \left\{\frac{\pi}{K_N(t;t)}\right\}^{\frac{1}{2}} \int_t^z K_N(\zeta;t)d\zeta, \tag{1.8}$$

to the mapping function f(z). We shall refer to this method of numerical conformal mapping as the Bergman kernel method (BKM) with basis $\{v_j(z)\}$.

The major shortcoming of the BKM is that the Gram-Schmidt process is usually numerically unstable; see Davis and Rabinowitz (1961;p.61). Thus, in practice, only a limited number of orthonormal functions $\phi_j(z)$ can be computed accurately and, for this reason, the success of the method depends strongly on the speed with which the series (1.3) converges. Since the convergence of (1.3) depends on the orthonormal basis used, it follows that the choice of an appropriate basis is of paramount practical importance.

The use of the BKM with the complete set $\{z^j\}_{j=0}^{\infty}$ as basic has been considered by Burbea (1970). Unfortunately the convergence of the series

$$K(z;t) = \sum_{j=1}^{\infty} p_j(z)\overline{p_j(t)}, \tag{1.9}$$

where the $p_j(z)$ are the polynomials obtained by orthonormalizing the powers $1, z, z^2, \ldots,$ is often extremely slow. This is

due to the presence of singularities of K(z;t), in the complement of Ω, which can affect seriously the rate of convergence of the series (1.9). For this reason the use of the set $\{z^j\}_{j=0}^{\infty}$ as a basis for the BKM does not lead to a practical method for the numerical mapping of Ω onto the unit disc.

In the present paper we consider using the set $\{z^j\}$ augmented by the introduction of appropriate singular functions, as a basis for the BKM. In section 2, we show that, in many cases, considerable information about the singularities of (z;t) is available. We use this information to construct an augmented basis, and a corresponding non-polynomial orthonormal set $\{\phi_j(z)\}$, for which the series (1.3) converges rapidly. In section 3, we present numerical results which indicate clearly that, if such an augmented basis is used, the BKM is an extremely efficient method for the numerical mapping of simply-connected domains.

2. Singularities of K(z;t) - Choice of Basis for the BKM.

In this section we consider two types of singularities of the Bergman kernel function K(z;t) on the complement of Ω, which affect the rate of convergence of the polynomial series in (1.9). These are either poles of K(z;t) which lie close to the boundary $\partial\Omega$ or branch point singularities on the boundary itself. We describe how available information about these singularities can be used to appropriately augment the basis set $\{z^j\}$ of the BKM, by introducing functions which reflect the main singular behaviour of K(z;t).

(i) Poles. To illustrate the damaging influence that the poles of K(z;t) can have upon the rate of convergence of the representation (1.9), we consider the trivial case of the mapping of the unit disc Ω_o onto itself. The function which effects this mapping so that the point $t \in \Omega_o$ is mapped onto the origin of the w-plane is

$$f(z) = (z-t)/(z-1/\bar{t}).$$

Thus, both f(z) and the corresponding Bergman kernel function K(z;t) have a pole at $z = 1/\bar{t}$. Since the polynomials

$$p_k(z) = \left[\frac{k}{\pi}\right]^{\frac{1}{2}} z^{k-1}, \qquad k = 1,2,....,$$

form a complete orthonormal set in Ω_o it follows that, in this case,

the polynomial series representation of K(z;t) is

$$K(z;t) = \frac{1}{\pi} \sum_{k=1}^{\infty} k(\bar{t}z)^{k-1}. \tag{2.1}$$

The series (2.1) converges rapidly when |t| is small, but the rate of convergence slows down considerably as $|t| \to 1$. In other words, the convergence of (2.1) is slow when the pole $z = 1/\bar{t}$ is near the boundary of Ω_o.

In general, the damaging influence that the poles of K(z;t) have upon the numerical process can be removed by introducing appropriate rational functions into the basis set $\{z^j\}$. In order to motivate a procedure for determining such an augmented basis, we consider the mapping of the rectangular domain

$$\Omega_{ab} = \left\{ (x,y) \;\middle|\; |x| < \frac{a}{2},\ |y| < \frac{b}{2} \right\}; \quad b \le a,$$

onto Ω_o. The mapping function is, in this case, known in terms of elliptic functions. However, it is more instructive, for our purpose, to determine the poles of the corresponding Bergman kernel function by considering the singularities of the Green's function of Ω_{ab}. For this we note that, in the general case, the mapping function f(z) in (1.4) is connected to the Green's function G(x,y;t) of Ω by

$$f(z) = \exp\{-2\pi(G(x,y;t) + i(x,y))\}, \tag{2.2}$$

where H(x,y) is the conjugate harmonic of G(x,y;t). Using the method of images it is possible to express the Green's function of Ω_{ab}, by an infinite double sum of logarithmic functions. In particular,

$$G(x,y;0) = \frac{1}{2\pi} \sum_{m,n=-\infty}^{\infty} (-1)^{m+n} \log \frac{1}{|z - z_{mn}|},$$

where $z_{mn} = ma + nbi$; see fig.2.1. Since the conjugate harmonic of $\log|z - z_{mn}|$ is arg $(z - z_{mn})$ it follows, from (2.2),

that the mapping function f(z) which maps Ω_{ab} onto Ω_o so that f(0) = 0 is given by

$$f(z) = \exp\left\{\sum_{m,n=-\infty}^{\infty}(-1)^{m+n}\,\mathrm{Log}(z-z_{mn})\right\}$$

$$= \left\{\prod_{m+n=\text{even}}(z-z_{mn})\right\} \Big/ \left\{\prod_{m+n=\text{odd}}(z-z_{mn})\right\} \qquad (2.3)$$

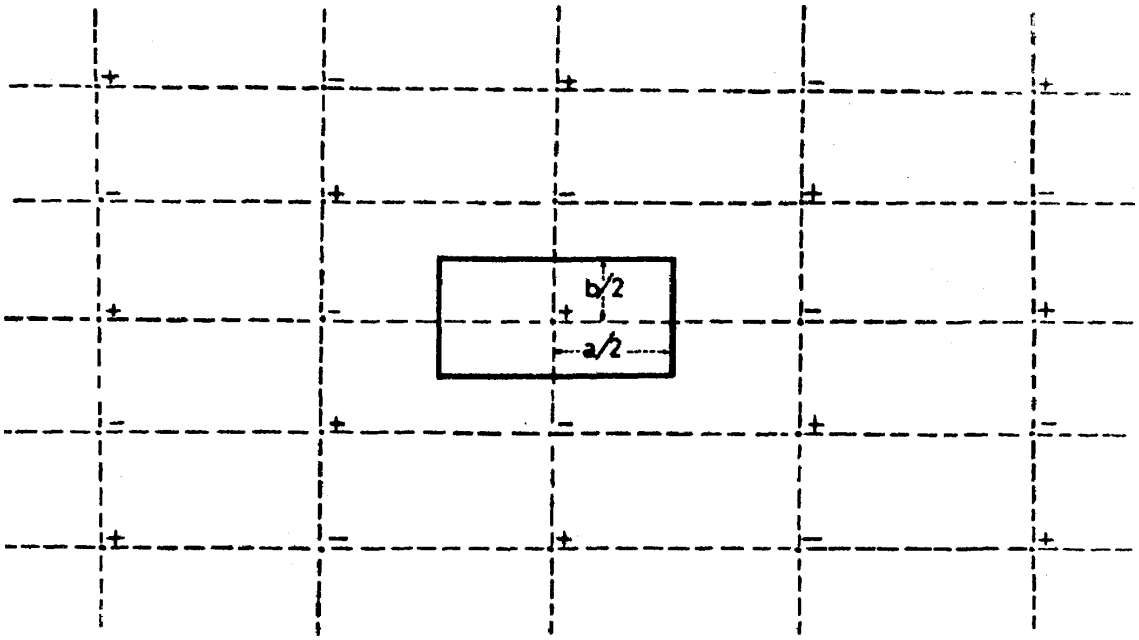

Figure 2.1

Thus, both f(z) and the corresponding kernel function K(z;0) have poles at all the "negative" images of the point t = 0, with respect to the four sides of Ω_{ab} (i.e. at all the points labeled with the - ve sign in fig. 2.1). The poles which have the most damaging effect on the convergence of the representation (1.9) are those at ±a and ±ib. These four poles bound the region of convergence of any polynomial series expansion of f(z) and affect the convergence of (1.9) even when Ω_{ab} is a square. However, their influence is much more damaging when Ω_{ab} is a thin rectangle.

This occurs because when b << a the distance of the poles ± ib from $\partial\Omega_{ab}$, is small relative to the dimensions of Ω_{ab}.

We note, from (2.3), that f(z) can be written as

$$f(z)\frac{z}{(z^2-a^2)(z^2+b^2)}\quad g(z),$$

where g(z) is analytic in the region

$$\left\{(x,y)\quad :\quad \left|\frac{x}{a}\right|+\left|\frac{y}{b}\right|<3\right\}.$$

Since, from (1.6),

$$K(z:0)=\left\{\frac{K(0:0)}{\pi}\right\}^{\frac{1}{2}}\quad f'(z),$$

it is natural to expect that the set

$$\left[\frac{z}{z-a}\right]',\ \left[\frac{z}{z+a}\right]',\ \left[\frac{z}{z-ib}\right]',\ \left[\frac{z}{z+ib}\right]',\qquad z^k,\ k=0,1,2,....,\tag{2.4}$$

where the prime denotes differentiation with respect to z, constitutes a more appropriate basis for the BKM than the set $\left\{z^k\right\}_{k=0}^{\infty}$. The choice of the set (2.4) as the basis for the BKM is justified completely by the numerical results of example 1, section 3.

In the general case, let the mapping function f(z) in (1.4) have a pole at z=p. Then, in order to remove the influence of this pole from the numerical process we augment the basis set $1,z,z^2,...,$ by introducing the function $\{(z-t)/(z-p)\}'$. As in the case of the rectangle, we construct the basis in this way by considering only the poles of f(z) that lie close to the boundary $\partial\Omega$ Thus, our procedure for determining a basis requires knowledge of the dominant poles of f(z) or equivalently, by equation (2.2), knowledge of the dominant singularities of the Green's function G(x,y;t) of Ω, in the complement of $\Omega u\partial\Omega$. For polygonal domains these singularities can be determined by the method of images. The method of images can also be used for some other domains whose boundaries are composed of straight line

segments and circular arcs. For domains involving more general curved boundaries no standard technique for determining the dominant singularities of G(x,y;t), and hence the corresponding poles of f(z), is available. However, if a good approximation $\tilde{p}$ to the pole of f(z) at z =p can be obtained, by some method, then the introduction of the function $\{(z-t)/(z-\tilde{p})\}'$ into the basis set is sufficient to remove the influence of the pole from the numerical process; see example 5, section 3.

(ii) Branch point singularities. Let the simply-connected domain Ω be partly bounded by two analytic arcs Γ_1 and Γ_2 which meet at the point z_o and form there a corner of interior angle $\alpha\pi$, where $\alpha = p/q > 0$ is a fraction reduced to lowest terms. Assume, without loss of generality, that in (1.5) $t = 0 \in \Omega$ and consider the asymptotic behaviour, in the neighbourhood of z_o, of the mapping function f(z) in (1.4).

For simplicity we consider first the case where Ω is a polygonal domain. Then, the Schwarz-Christoffel formula shows that, in the neighbourhood of z_o,

$$f(z) - f(z_o) = \sum_{k=1}^{\infty} a_k (z - z_o)^{k/\alpha} ,$$

or, since f(0) =0,

$$f(z) = \sum_{k=1}^{\infty} a_k \left\{ (z - z_o)^{k/\alpha} - (-z_o)^{k/\alpha} \right\} ; \qquad (2.5)$$

see e.g. Copson (1975;p.70). Thus, for $\alpha \neq 1/q$, the asymptotic expansion of f(z) involves fractional powers of $(z-z_o)$. That is unless $1/\alpha$ is an integer, both f(z) and the corresponding kernel function have a branch point singularity at z_o which always affects the rate of convergence of (1.9), particularly in the neighbourhood of z_o This singularity becomes more pronounced as the angle $\alpha\pi$ increases and if $\alpha > 1$, i.e. if the corner is re-entrant, its effect upon the accuracy of the numerical process is catastrophic; see examples 3, 4 and 7, section 3.

As in the case of a pole, we expect that the use of a basis with terms that reflect the main singular behaviour of the

Bergman kernel function, in the neighbourhood of z_o, will remove the damaging influence of a branch point singularity at z_o. Thus, we augment the basis set 1, z, z^2,..., by introducing the functions

$$(z-z_o)^{k/\alpha-1} \quad , \tag{2.6}$$

corresponding to the first few singular terms of (2.5).
The choice of such an augmented set as a basis for the BKM is completely justified by the numerical results of examples 2,3,4 and 7.

If Ω is a non-polygonal domain then the asymptotic expansion of f(z) can be deduced from the results of Lehman (1957). These results, which include (2.5) as a special case, show that in the neighbourhood of z_o,

$$f(z)-f(z_o) = (z-z_o)^{1/\alpha} M\{(z-z_o), (z-z_o)^{1/\alpha}, (z-z_o)^q \log(z-z_o)\} \tag{2.7}$$

where M is a triple power series in its arguments. The expansion (2.7) differs from (2.5) in that apart from powers of $(z-z_o)$ it also involves logarithmic terms of the form

$$(z-z_o)^{\beta}\{\log(z-z_o)\}^m; \tag{2.8}$$

where m is an integer. Thus, for a non-polygonal domain, we cannot conclude that there is no singularity at z_o, even when $\alpha=1/q$. The reason for this is that logarithmic terms may be present in (2.7). For any value of α the dominant singular functions required for the augmentation of the basis can be determined from (2.7).

Two difficulties arise if functions of the form (2.6), (2.8) are included in the basis. The first concerns the number of singular functions that should be included. Our experiments show that, after a certain value, a further increase in the number of singular functions improves the accuracy of the mapping in the neighbourhood of the corner but destroys some of the accuracy elsewhere in the domain. Our criterion for choosing the "optimum" number is based on intuitive arguments and,

unfortunately, we cannot state a general rule. The second difficulty concerns the computation of the inner products required for the Gram-Schmidt process. This however does not present serious problems and it can often be overcome by a very simple technique; see the remarks in section 3.

3. Numerical Examples

In all the examples considered in this section the augmented basis is formed by introducing into the set $\{z^j\}$ appropriate singular functions, as described in section 2.

The orthonormalization of the basis set $\{v_j(z)\}_{j=1}^{N}$, by means of the Gram-Schmidt process, requires the evaluation of the inner products

$$(v_m(z), v_n(z)) = \iint_\Omega v_m(z)\overline{v_n(z)}\, dxdy \quad , \quad m,n = 1,2...., N.$$

Using Green's formula the inner products are expressed in the form

$$(v_m(z), v_n(z)) = \frac{1}{2i}\int_{\partial\Omega} v_m(z)\overline{v_n(z)}\, dz \quad ; \quad V_n'(z) = v_n(z), \qquad (3.1)$$

and, as in Burbea (1970), the integrals in (3.1) are computed by Gaussian quadrature. If, due to the presence of a corner, the basis set contains functions of the form (2.6) or (2.8) then the Gauss-Legendre quadrature formula may fail to produce sufficiently accurate approximations to the inner products which involve these singular functions. It is then necessary to use special techniques in order to improve the accuracy of the quadrature. These techniques depend on the geometry of $\partial\Omega$ and, for this reason, it is not possible to describe a procedure for a general $\partial\Omega$. If however, as is frequently the case, the arms Γ_1, Γ_2 of the corner z_o under consideration are both straight line segments then the singularities of the integrands can always be removed by choosing an appropriate parametric representation for 3ft. Assume, for example, that the interior angle of the corner at z_o is $p\pi/q$, $p \neq 1$ and, as a result, the augmented basis involves terms of the form $(z - z_o)^{(kq-p)/p}$ Then, in order to remove the singularities due to the fractional powers in the

integrands we choose the parametric representations of Γ_1 and Γ_2 to be respectively

$$z = a_k t^p \exp(i\theta_k) + z_o, \qquad z \in \Gamma_k, \qquad k = 1,2. \tag{3.2}$$

In (3.2) $\tan\theta_k$, k = 1,2 are respectively the gradients of the straight lines Γ_1 and Γ_2 and a_k, k =1,2 are real constants chosen so that Γ_1 corresponds to the interval $t_1 \le t \le 0$ and Γ_2 to the interval $0 \le t \le t_1$. If, apart from fractional powers of $(z - z_o)$, the basis also involves logarithmic terms then the effect of the integrand singularities can be suppressed by taking the parametric representations of Γ_1 and Γ_2 to be respectively

$$z = a_k t^n \exp(i\theta_k) = z_o, \quad z \in \Gamma_k, \quad k = 1,2. \tag{3.3}$$

when n is a sufficiently large positive integer.

In all the examples we take t = 0 in (1.5). Thus, once the orthonormal set $\{\phi_j(z)\}_{j=1}^{N}$, corresponding to the basis set $\{v_j(z)\}_{j=1}^{N}$ is constructed we form the sum

$$K_N(z;0) = \sum_{j=1}^{N} \phi_j(z)\overline{\phi_j(0)}$$

and hence, using (1.8), we obtain by formal integration the approximation $f_N(z)$ to the mapping function f(z).

For every simply-connected domain considered, and for every choice of basis, the numerical results given correspond to the approximation $f_{N_{opt}}(z)$ This approximation is opt determined as follows. In each case a sequence of approximations $\{f_n(z)\}$ is computed by taking $N = N_{min}, N_{min} + 1, N_{min} + 2,...,$ where N_{min} denotes the smallest number of basis functions used. At each stage the quality of the approximation $f_N(z)$ is determined by computing

$$e_N(z) = 1 - \left| f_N(z) \right|$$

at M" boundary test points" $z_j \in \partial\Omega$, $j = 1,2,...,M$.

The quantity

$$E_N = \max_j \left| e_N(z_j) \right|$$

then gives an estimate of the maximum error in the modulus of $f_N(z)$. If at the (N+l) th stage the inequality

$$E_{N+1} < E_N \tag{3.4}$$

is satisfied then the number of basis functions is increased by one and the approximation $f_{N+2}(z)$ is computed. When for a certain value of N, due to numerical instability, the inequality (3.4) no longer holds we terminate the process and take this value of N to be the optimum number N_{opt} of basis functions.

For each example we list the augmented basis, the boundary test points and the order of the Gaussian quadrature used. Also, when the accurate computation of the inner products requires the use of a special parametric representation for part of the boundary $\partial\Omega$, we give this representation.

In presenting the results we denote the BKM with monomial basis $\{z^{(j-1)}\}_{j=1}^{N}$ by BKM/MB and the BKM with augmented basis by BKM/AB.

All computations were carried out, in single length arithmetic, on a CDC 7600 computer.

EXAMPLE 1

Rectangle $\{(x,y) : |x| \le a, |y| \le 1\}$; Fig .3.1

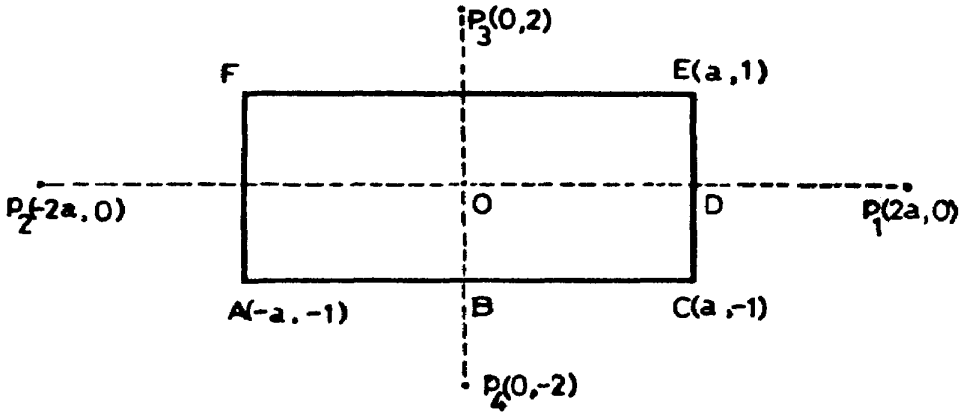

Figure 3.1

Augmented Basis. Because the domain has fourfold symmetry about the origin, odd powers of z do not appear in the polynomial representation of the kernel function K(z;0) see Burbea (1970, p.824). For this reason, when $a \neq 1$, we take the monomial basis set to be $\{z^{2(j-1)}\}_{j=1}^{N}$. When a = 1 the domain has eightfold symmetry and the polynomial representation of K(z;0) includes only powers of z which are multiples of 4. In this case we take the monomial basis to be $\{z^{4(j-1)}\}_{j=1}^{N}$.

The augmented basis is formed by introducing into the monomial basis the four singular functions corresponding respectively to the four poles at z = ±2a and z=±2i. The symmetry of the domain implies that these four singular functions can be combined into the two functions $\{z/(z^2-4a^2)\}'$ and $\{z/z^2+4)\}'$. A further simplification occurs when a = 1. In this case the four singular functions can be combined into the single function $\{z/(z^4-16)\}'$. Thus, the augmented basis is

$$v_1 = \left\{\frac{z}{z^2-4a^2}\right\}', \quad v_2 = \left\{\frac{z}{z^2+4}\right\}', \quad v_{j+3} = z^{2j}, \quad j = 0,1,2,...., \quad \text{when } a \neq 1,$$

and

$$v_1 = \left\{\frac{z}{z^4-16}\right\}', \quad v_{j+2} = z^{4j}, \quad j = 0,1,2,....; \quad \text{when } a = 1.$$

Quadrature. Gauss-Legendre formula with 48 points along each side of the rectangle.

Boundary Test Points. Because of the symmetry, we only consider points on AC and CE. The points are distributed in steps of a/5 and 0.2 along AC and CE respectively, starting from A.

Numerical Results. See Tables 3.1(a) and 3.1(b).

TABLE 3.1(a)

Values of N_{opt} and $E_{N_{opt}} = \max_j \left| e_{N_{opt}}(z_j) \right|$

a	BKM/MB		BKM/AB	
	N_{opt}	$E_{N_{opt}}$	N_{opt}	$E_{N_{opt}}$
1	9	1.4×10^{-8}	5	3.4×10^{-11}
2	17	2.1×10^{-5}	10	2.1×10^{-10}
6	13	4.1×10^{-2}	10	1.9×10^{-6}

TABLE 3.1(b)

Values of $e_{N_{opt}}(z)$ at a selection of boundary points: see Fig.3.1

POINT	a = 1		a = 2		a = 6	
	BKM/MB	BKM/AB	BKM/MB	BKM/AB	BKM/MB	BKM/AB
A	1.2×10^{-8}	3.4×10^{-11}	2.1×10^{-5}	7.2×10^{-11}	4.1×10^{-2}	1.7×10^{-7}
B	1.4×10^{-8}	6.7×10^{-12}	1.5×10^{-5}	7.0×10^{-11}	3.3×10^{-2}	1.9×10^{-6}
C	1.2×10^{-8}	3.4×10^{-11}	2.1×10^{-5}	2.1×10^{-10}	4.1×10^{-2}	1.2×10^{-7}
D	1.4×10^{-8}	6.7×10^{-12}	1.9×10^{-5}	2.0×10^{-10}	4.4×10^{-2}	8.0×10^{-7}

EXAMPLE 2

Quadrilateral; Fig 3.2

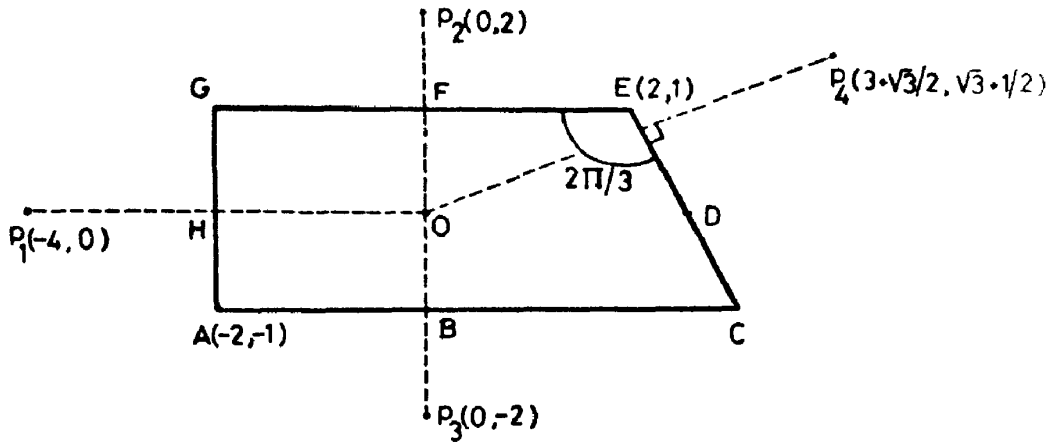

Figure 3.2

Augmented Basis

$$v_j = \left\{ \frac{z}{z - p_j} \right\}' , \quad j = 1,2,3,4; \quad v_5 = 1, \quad v_6 = (z - z_E)^{\frac{1}{2}}, \quad v_7 = z, \quad v_8 = z^2$$

$$v_9 = (z - z_E)^{7/2} , \; v_{9+j} = z^{2+j} , \quad j = 1,2,3, \; ....,$$

Quadrature. Gauss-Legendre formula with 48 points along each side of the quadrilateral.

In order to perform the integration accurately we choose the parametric representation of CE and EG to be of the form (3.2). Thus, we take,

$$z = \begin{cases} (2 + 1/\sqrt{3})t + z_A & , \quad 0 \le t \le 2; \text{ for AC} \\ -\frac{4}{\sqrt{3}} (t-3)^2 \exp\left(\frac{2\pi i}{3}\right) + z_E & , \quad 2 \le t \le 3; \text{ for CE} \\ -(t-3)^2 + z_E & , \quad 3 \le t \le 5; \text{ for EG} \\ -2(t-6)\, i + z_A & , \quad 5 \le t \le 6; \text{ for GA} \end{cases} \qquad (3.5)$$

Boundary Test Points. The distribution of the points is defined by (3.5) with t = 0(0.25)6,

Numerical Results.

For the BKM/MB, N_{opt} and $E_{21} = 2.2\times10^{-3}$.

For the BKM/AB, N_{opt} and $E_{17} = 5.2\times10^{-7}$.

Values of $\left|e_{N_{opt}}(z)\right|$ at a selection of boundary points are given in Table 3.2.

TABLE 3.2

POINT	BKM/MB	BKM/MB
A	1.9×10^{-3}	4.3×10^{-7}
B	1.7×10^{-3}	2.6×10^{-7}
C	1.3×10^{-4}	4.7×10^{-7}
D	2.3×10^{-4}	1.5×10^{-7}
E	1.1×10^{-3}	4.6×10^{-7}
F	1.2×10^{-3}	2.0×10^{-7}
G	1.8×10^{-3}	8.7×10^{-8}
H	1.0×10^{-3}	1.7×10^{-7}

EXAMPLE 3

L - shaped region ; Fig.3.3

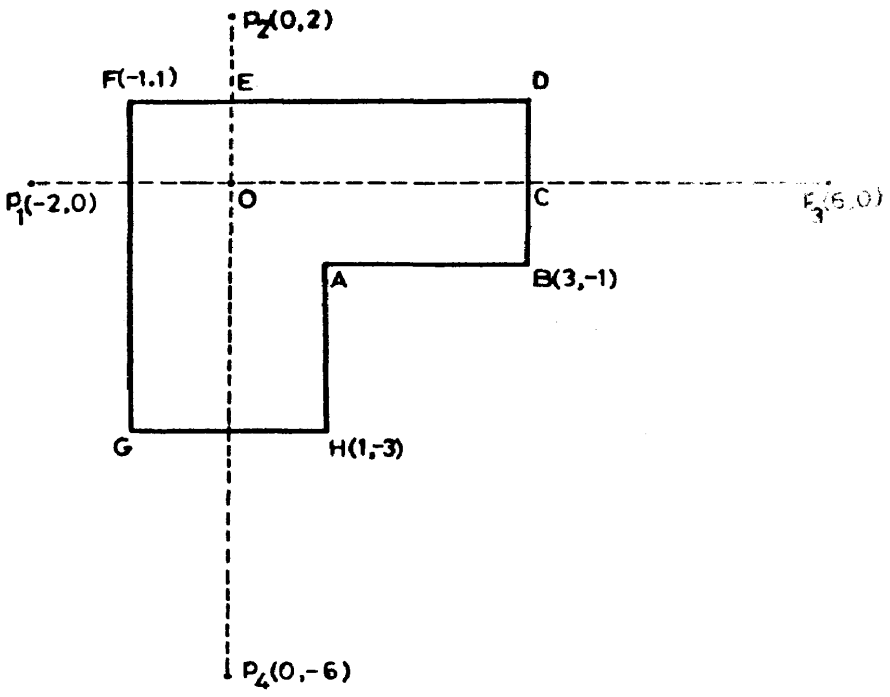

Figure 3.3

Augmented Basis.

$$v_j = \left\{ \frac{z}{z - p_j} \right\}' , \quad j = 1,2,3,4,; \quad v_5 = (z - z_A)^{-1/3}, \quad v_6 = 1, \quad v_7 = (z - z_A)^{1/3}$$

$$v_8 = z, \quad v_9 = (z - z_A)^{5/3}, \quad v_{10} = z^2, \quad v_{11} = (z - z_A)^{7/3}, \quad v_{12} = z^3,$$

$$v_{13} = (z - z_A)^{11/3}, \quad v_{13+j} = z^{3+j}, \quad j = 1,2 \ldots .,$$

Quadrature. Gauss-Legendre formula with 16 points along each side of the polygon.

In order to perform the integration accurately we choose the parametric representations of HA and AB to be the form (3.2). Thus,

we take,

$$z = \begin{cases} \frac{i}{4}\, t^3 + z_A \quad , & -2 \le t \le 0; \quad \text{for HA} \\ \frac{1}{4}\, t^3 + z_A \quad , & 0 \le t \le 2; \quad \text{for AB} \end{cases} \tag{3.6}$$

Boundary Test Points. On each of the sides BD,DF,FG and GH the points are equally spaced, in steps of 0.25, starting from a corner. On HA and AB the distribution of the points is defined by (3.6) with t = -2(0.25)2.

Numerical Results.

For the BKM/MB, $No_{opt} = 24$ and $E_{24} = 1.9\times10^{-1}$.

For the BKM/AB, N_{pot}, $= 26$ and $E_{26} = 2.2\times10^{-5}$.

Values of $|e_{N_{opt}}(z)|$ at a selection of boundary points are given in Table 3.3.

TABLE 3.3

POINT	BKM/MB	BKM/MB
A	1.9×10^{-1}	2.2×10^{-5}
B	1.9×10^{-1}	1.1×10^{-5}
C	8.8×10^{-2}	3.2×10^{-6}
D	1.8×10^{-2}	1.1×10^{-5}
E	2.0×10^{-2}	7.9×10^{-6}
F	3.0×10^{-2}	2.2×10^{-5}

Example 4

Octagon ; Fig.3.4

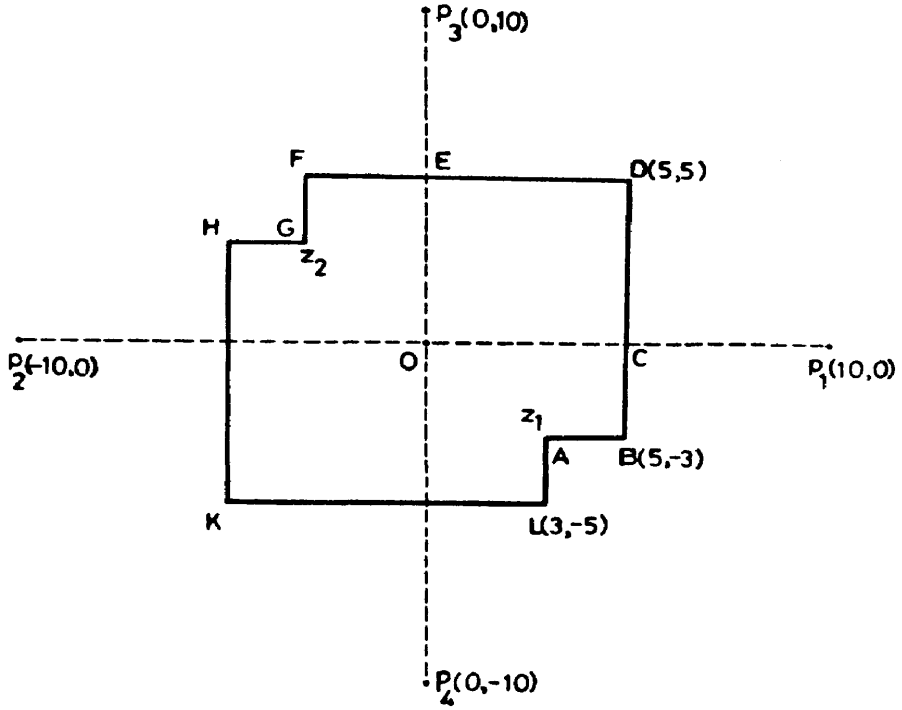

Figure 3.4

Augmented Basis. Because the domain has fourfold symmetry about the origin, the monomial basis set is taken to be $\left\{ z^{2(j-1)} \right\}_{j-1}^{N}$. The augmented basis used is,

$$v_1 = \left\{ \frac{z}{z^2 - 100} \right\}', \quad v_2 = \left\{ \frac{z}{z^2 + 100} \right\}', \quad v_{2+j} = (z - z_j)^{-1/3}, \quad j = 1, 2;$$

$$v_5 = 1, v_{5+j} = (z - z_j)^{1/3}, \quad j = 1,2; \quad v_{7+j} = (z - z_j)^{5/3}, \quad j = 1,2;$$

$$v_{10+j} = z^{2j}, \quad j = 1,2, \ldots .$$

Quadrature. Gauss-Legendre formula with 16 points along each side of the polygon.

In order to perform the integration accurately we choose the parametric representations of LA,AB,FG and GH to be of the form (3.2). Thus, we take

$$z = \begin{cases} 2it^3 + z_1 , & -1 \le t \le 0; \text{ for LA,} \\ 2\,t^3 + z_1 , & 0 \le t \le 1; \text{ for AB,} \end{cases} \tag{3.7}$$

and similar representations for FG and GH.

Boundary Test Points. On each of the sides BD, DF, HK and KL the points are equally spaced, in steps of 1.0, starting from a corner. On LA and AB the distribution of the points is defined by (3.7) with t =-1(0.25)1. On FG and GH the distribution is similar to that on LA and AB.

Numerical Results

For the BKM/MB, $N_{opt} = 27$ and $E_{27} = 1.3\times10^{-1}$.

For the BKM/AB, $N_{opt} = 23$ and $E_{23} = 5.7\times10^{-6}$.

Values of $\left|e_{N_{opt}}(z)\right|$ at a selection of boundary points are given in Table 3.4.

TABLE 3.4

POINT	BKM/MB	BKM/MB
A	1.3×10^{-1}	2.1×10^{-6}
B	4.9×10^{-3}	5.0×10^{-6}
C	5.3×10^{-3}	3.5×10^{-6}
D	5.4×10^{-3}	5.7×10^{-6}
E	5.3×10^{-3}	5.0×10^{-6}
F	4.9×10^{-3}	5.1×10^{-6}
G	1.3×10^{-1}	2.1×10^{-6}

EXAMPLE 5

Ellipse $\{(x, y) : \frac{x^2}{a^2} + y^2 \leq 1\}$.

Augmented Basis. Because the domain has fourfold symmetry about the origin the monomial basis set is taken to be $\{z^{2(j-1)}\}_{j=1}^{N}$.

The mapping function f(z) is, in this case, given by an elliptic sine; see e.g. Kober (1957;p.177). From this we find that the of f(z) nearest to the boundary occur at $z = \pm ip, 2a^2/(a^2-1)$. the augmented basis is

$$v_1 = \left\{\frac{z}{z^2+p^2}\right\}', \quad v_{j+1} = z^{2(j-1)}, \quad j = 1,2,.... \tag{3.8}$$

We also perform the BKM/AM with basis

$$v_1 = \left\{\frac{z}{z^2+\tilde{p}^2}\right\}', \quad v_{j+1} = z^{2(j-1)}, \quad j = 1,2,.... \tag{3.9}$$

where $\tilde{p} = (2a^2-1)/(a^2-1)$. This corresponds to approximating the poles at $\pm ip$ by $\pm i\tilde{p}$, where $(0, \tilde{p})$ is the inverse point of the origin with respect to the circle of curvature of the ellipse at the point (0, 1).

Quadrature. Gauss-Legendre formula with 48 points along each of the four subarcs defined respectively by

$$x = a\cos t, \; y = \sin t \tag{3.10}$$

with $j\frac{\eta}{2} \leq t \leq (j+1)\frac{\pi}{2}$, $j = 0,1,2,3$.

Boundary Test Points. The points are defined by (3.10) with $t = 0\left(\frac{\pi}{8}\right) 2\pi$.

Numerical Results. See Table 3.5.

TABLE 3.5

Values of N_{opt} and $E_{N_{opt}} = \max_j \left| e_{N_{opt}}(z_j) \right|$

a	BKM/MB		BKM/AB Basis (3.8)		BKM/AB Basis (3.8)	
	N_{opt}	$E_{N_{opt}}$	N_{opt}	$E_{N_{opt}}$	N_{opt}	$E_{N_{opt}}$
2.5	13	2.6×10^{-5}	6	3.5×10^{-11}	12	3.1×10^{-7}
5.0	11	1.0×10^{-2}	11	3.3×10^{-10}	12	2.5×10^{-6}
10.0	11	9.4×10^{-2}	11	5.8×10^{-6}	11	7.3×10^{-6}
20.0	11	2.8×10^{-1}	11	5.6×10^{-4}	11	5.5×10^{-4}

EXAMPLE 6

Simply - connected region,

$\{(x,y): -1 \le x \le 0,\ |y| \le 1\} \cup \{(x,y): x^2 + y^2 \le 1\}$; Fig. 3.5

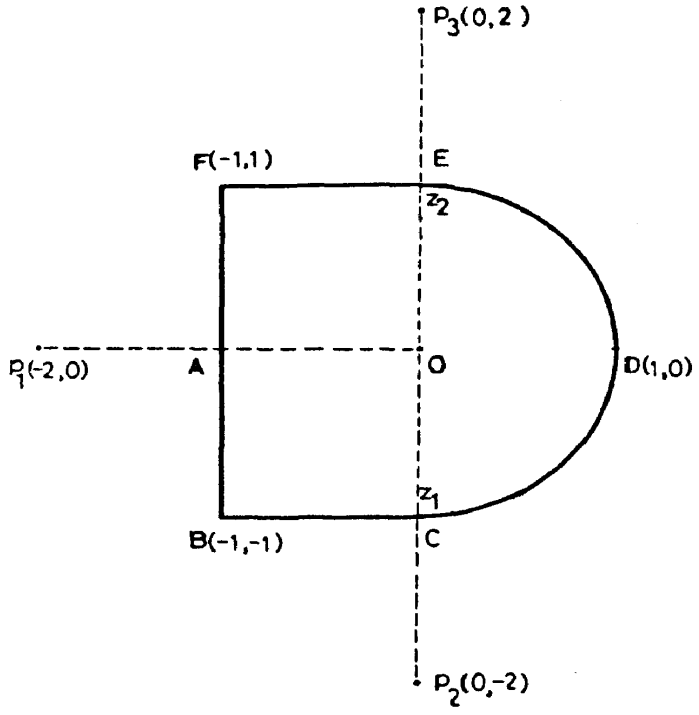

Figure 3.5

Augmented Basis

$$v_j = \left\{ \frac{z}{z - p_j} \right\}' \quad , \quad j = 1,2,3; \; v_4 = 1, \; v_{4+j} = \{(z - z_j)^2 \log(z - z_j)\}' \; , j = 1,2;$$

$$v_7 = z, \quad v_{7+j} = \{(z - z_j)^3 (\log(z - z_j))^2\}' \quad , \quad j = 1,2;$$

$$v_{9+j} = z^{1+j} \quad , \quad j = 1,2, \; ....$$

Quadrature. Gauss-Legendre formula with 48 points along each of the straight lines BC,EF,FB and the arcs CD,DE.

In order to perform the integration accurately we choose the parametric representation of BC and EF to be of the form (3-3) with n =10. We also take the parametric representation of the semi-circle CDE to be

$$t^{10}(2 - t^{20})^{\frac{1}{2}} - i(1 - t^{20}) \quad , \quad 0 \le t \le 1 \text{ ; for CD}$$

$$(2 - t)^{10}\{2 - (2 - t)^{20} + i\{1 - (2 - t)^{20}\} \quad , \quad 1 \le t \le 2 \text{ ; for DE.}$$

Boundary Test Points. On each of the straight lines FB, BC, FE the points are equally spaced, in steps of 0.25, starting from a corner. On the semi-circle CDE the distribution of the points is defined by

$$z = e^{it} \; , \; t = -\frac{\pi}{2}\left(\frac{\pi}{8}\right)\frac{\pi}{2} .$$

Numerical Results

For the BKM/MB, $N_{opt} = 20$ and $E_{20} = 5.5 \times 10^{-4}$.

For the BKM/AB, $N_{opt} = 26$ and $E_{26} = 1.5 \times 10^{-6}$.

Values of $|e_{N_{opt}}(z)|$ at a selection of boundary points are given in Table 3.6

TABLE 3.6

POINT	BKM/MB	BKM/MB
A	1.9×10^{-4}	4.2×10^{-7}
B	5.5×10^{-4}	6.7×10^{-7}
C	1.9×10^{-4}	1.5×10^{-6}
D	1.4×10^{-4}	2.6×10^{-8}

EXAMPLE 7

Circular sector of radius 1 and angle 3π/2; Fig. 3.6

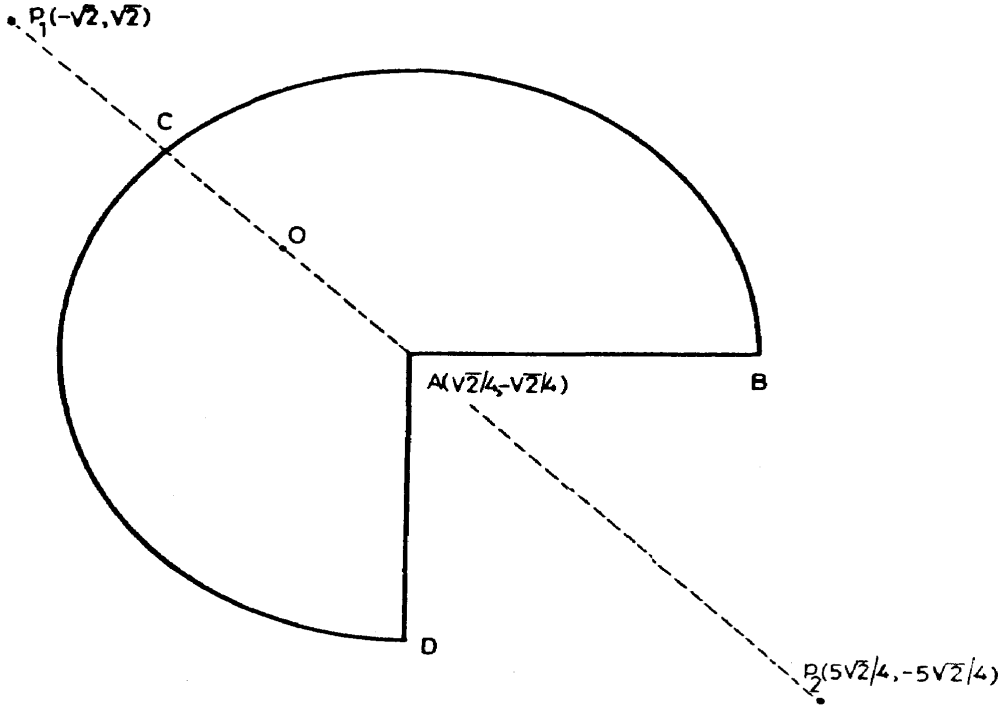

Figure 3.6

Augmented Basis.

$$v_j = \left\{ \frac{z}{z-P_j} \right\}' \quad , \quad j=1,2; \quad v_3 = (z-z_A)^{-1/3} \quad , \quad v_4 = 1, v_5 = (z-z_A)^{1/3} \quad ,$$

$$v_6 = z, \; v_7 = (z-z_A)^{5/3}, \; v_8 = z^2, \; v_9 = (z-z_A)^{7/3}, \; v_{10} = z^3,$$

$$v_{11} = (z-z_A)^{11/3}, \; v_{11+j} = z^{3+j} \quad , \quad j=1,2,....$$

Quadrature. Gauss-Legendre formula with 48 points along each of the straight lines AB, AD and the arcs BC, CD.

In order to perform the integration accurately the parametric representations of DA and AB are chosen to be of the form (3.2).

Boundary Test Points. On each of AB and AD the points are equally spaced, in steps of 0.25, starting from a corner. On the are BCD the distribution of the points is defined by $z = z_A + e^{it}$, $t = 0\left(\frac{\pi}{4}\right)\frac{3\pi}{2}$.

Numerical Results.

For the BKM/MB, $N_{opt}=21$ and $E_{21}=|e_{21}(z_A)|=1.7\times10^{-1}$.

For the BKM/AB, $N_{opt}=21$ and $E_{21}=|e_{21}(z_c)| =5.6\times10^{-5}$.

In table 3.7 we give the real and imaginary parts of the approximation $f_{21}(z)$ obtained by the BKM/AM at a selection of boundary and interior points. We compare these results with their analytic counterparts computed from the exact mapping function f(z).

TABLE 3.7

Key to point numbers

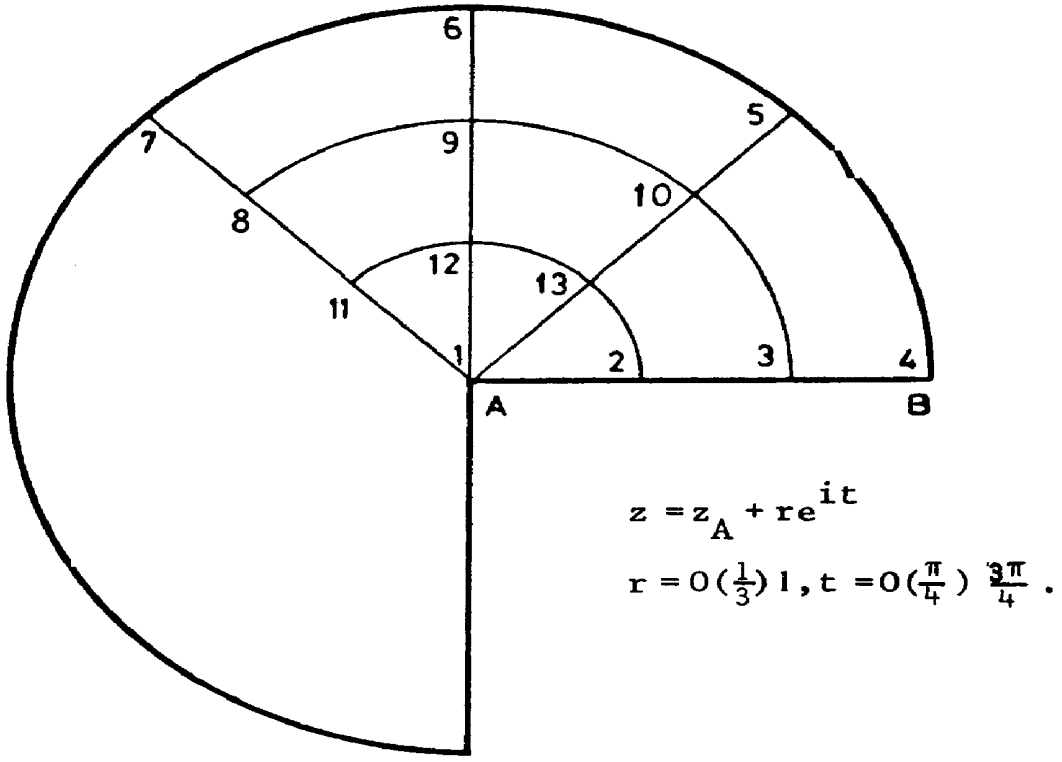

POINT	Real f_{21} (z)	Imag f_{21} (z)	Real f (z)	Imag f (z)
1	0.7070742	-0.7070742	0.7071068	-0.7071068
2	0.9975213	-0.0697145	0.9975633	-0.0697674
3	0.9968618	0.0797509	0.9968206	0.0796781
4	0.9941923	0.1075205	0.9942209	0.1073533
5	0.9748706	0.2226125	0.9748945	0.2226674
6	0.7371164	0.6756825	0.7371724	0.6757047
7	-0.7071362	0.7071362	-0.7071068	0.7071068
8	0.8684045	0.1575020	0.8684044	0.1575022
9	0.5360579	0.3627624	0.5360580	0.3627624
10	-0.1927762	0.1927762	-0.1927761	0.1927761
11	-0.7850148	-0.0348388	0.7850147	-0.0348398
12	0.5053199	-0.0187851	0.5053199	-0.0187850
13	0.1775234	-0.1775234	0.1775234	-0.1775234

4. Discussion.

The results of section 3 indicate clearly that in applying the BKM the choice of basis is of paramount importance. For the successful application of the method the basis set must contain terms which reflect the main singular behaviour of the kernel function. Provided that such a basis can be constructed the BKM is an extremely accurate method for the numerical conformal mapping of simply-connected domains.

For the rectangles and ellipses of examples 1 and 5 a direct comparison can be made between the BKM results and those obtained by other methods of numerical conformal mapping. For these domains the BKM/AM results are several orders of magnitude more accurate than those obtained by Rabinowitz(1966), using the Szegö kernel function method with orthonormal polynomials, and by Symm (1966), using an integral equation method. Also, for these domains, the BKM/AM approximations are as good as, or better than, those obtained by Hayes, Kahaner and Kellner (1972), who modified Symm's method in order to improve its accuracy.

The above three papers do not contain results obtained from the mapping of domains with sharp corners, like the domains of examples 3, 4 and 7. However, an indication of the poor performance of the integral equation methods for numerical conformal mapping, in the neighbourhood of a re-entrant corner, is given by the results of Symm (1974;p.273). For the L - shaped region of example 3, Symm's method yields an approximation $\tilde{f}(z)$ which at the re—entrant corner A has modulus $|\tilde{f}(z_A)| = 0.959$. Although the accuracy of $\tilde{f}(z)$ improves considerably away from the corner, at a boundary point distant $\frac{1}{4}$ AB from A the error in the modulus is still $|e(z_A)| = 5 \times 10^{-3}$. By contrast the BKM, with an appropriate augmented basis, overcomes the difficulties associated with sharp corners and produces accurate results throughout the region.

REFERENCES

BURBEA, J. 1970 Maths.Comput. 24, 821.

COPSON, E. T. 1975 Partial Differential Equations. London: Cambridge University Press.

DAVIS, P. J. & RABINOWITZ, P. 1961 In Advances in Computers Vol.2. (Ed.Franz.L.Alt), p.55. London and New York:Academic Press.

HAYES, J.K. KAHANER,D. K. & KELLNER, R. G. 1972 Maths.Comput. 26,327,

KOBER, H. 1957 Dictionary of Conformal Representations. New York: Dover.

LEHMAN, R.S. 1957 Pacific J. Math. 7 1437.

NEHARI, Z. 1952 Conformal Mapping. New York: McGraw-Hill.

RABINOWITZ, P. 1966 J.Assoc.Comput.Mach. 13 296.

SYMM, G.T. 1966 Num. Math. 9, 250.

SYMM, G.T. 1974 Numerical Solution of Integral Equations (Ed.L.M.Delves and J. Walsh) p.267, Oxford: Clarendon Press.